JOURNAL OF SOLID STATE CHEMISTRY 102, 69–78 (1993)

Synthesis and Characterization of a New Modification of the Quasi-Low-Dimensional Compound KMo_4O_6

K. V. RAMANUJACHARY AND M. GREENBLATT

Department of Chemistry, Rutgers, The State University of New Jersey, Piscataway, New Jersey 08855–0939

AND E. B. JONES AND W. H. McCARROLL

Chemistry Department, Rider College, POB 6400, Lawrenceville, New Jersey 08648

Received January 9, 1992; in revised form May 19, 1992; accepted May 20, 1992

Prismatic single crystals, up to 3 mm in length, of a third modification of KMo_4O_6 have been prepared by electrolysis of a melt with a high ratio of K_2MoO_4 to MoO_3. Single-crystal X-ray diffraction analysis shows that the structure conforms more closely than the other two modifications to that reported originally for $NaMo_4O_6$. When current is passed parallel to the tetragonal c axis (i.e., parallel to the *trans*-edge-sharing chains of Mo_6 octahedra) the compound displays metallic conductivity down to 100 K, where a broad transition to semiconducting behavior occurs. If the current is passed perpendicular to the c axis the conductivity is approximately a factor of 5 lower. Magnetic susceptibility measurements on a randomly oriented collection of crystals showed Pauli paramagnetic behavior with a small Curie tail at low temperatures. © 1993 Academic Press, Inc.

Introduction

Although there is a great deal of interest in materials with quasi-low-dimensional properties, the ability to characterize them properly is limited by the fact that single-crystal specimens of a size necessary for the measurement of their electrical, magnetic, and optical properties are often difficult to obtain. Perhaps the most notable exceptions to this observation are the alkali-metal molybdenum oxide bronzes about which a wealth of information exists because large single crystals can be obtained readily by fused salt electrolysis or by the temperature gradient flux growth method (*1–3*).

In contrast, very little is known about the physical properties of an interesting class of structurally low-dimensional low-valent molybdenum oxides containing infinite chains of *trans*-edge-sharing Mo_6 octahedra. The first report of such compounds was by Torardi and McCarley for the compound $NaMo_4O_6$ (*4, 5*). Subsequently a number of related compounds of Li, Ca, Ba, In, Sn, Zn, and Mn, among others, all of which contain similar Mo–Mo bonded chains, have been described by McCarley and co-workers (*6–10*). Recently, the synthesis and structures of the high- and low-pressure forms of KMo_4O_6 have been reported (*11*). The crystal structure of the former is closely related to that of $NaMo_4O_6$ but with significantly longer Mo–Mo distances parallel to

0022-4596/93 $5.00

the chain axis; the latter is described by the subcell reported for $Ba_{0.62}Mo_4O_6$ (*6, 10*). Theoretical studies of these extended chain compounds predict that their electronic properties should indeed be highly anisotropic (*12*). No detailed measurements of the electrical and magnetic properties of any of these compounds have been presented although McCarley *et al.* state that single-crystal resistivity measurements on In Mo_4O_6 and $Ca_{5.45}Mo_{18}O_{32}$ show that these compounds display metallic and semiconducting behavior, respectively, over a wide range of temperatures (*9*).

Since one of the long-term goals of our laboratories has been to prepare single crystals of reduced transition metal oxides with potentially interesting electrical and magnetic properties, we initiated a study to see if ternary oxide formation was possible using fused salt electrolysis when the ratios of alkali-metal molybdate to molybdenum(VI) oxide were considerably higher than those reported for the synthesis of alkali molybdenum oxide bronzes (*2, 13*). We herein report the successful synthesis of large (i.e., ~1 mm^3) single crystals of KMo_4O_6 by this method, which represent a third structural form of this compound whose Mo–Mo distances more closely correspond to those reported for $NaMo_4O_6$ (*11*). Measurements of their electrical conductivity and magnetic susceptibilities as a function of crystal orientation are also presented.

Experimental

Synthesis, Powder X-Ray Diffraction, and Elemental Analysis

The crystals used in these experiments were synthesized by the electrolysis of a melt obtained from a mixture of potassium molybdate and molybdenum(VI) oxide having a molar ratio of $K_2MoO_4 : MoO_3 = 6 : 1$. The anhydrous potassium molybdate was obtained by drying the reagent-grade dihydrate for 48 hr at 160°C, and reagent-grade MoO_3 was fired for 24 hr at 450°C in air before use. The electrolysis was carried out in air using a charge of 35–40 g contained in a 25-cm^3 McDanel 997 high-density alumina crucible. The cathode cell was partially isolated from the anode cell by a slotted alumina cylinder placed in the center of the crucible. The inner cell served as the cathode compartment. The anode was a 2-cm^2 platinum foil and the cathode was a small spiral platinum wound from 0.020-in.-diameter wire. A current of 20–25 mA was used for a period of 65 hr at a temperature of 930°C. Typically, runs were terminated by removing the electrodes from the melt and allowing them to cool rapidly to room temperature. The crystals, which grow in the form of black square prisms up to 3 mm in length and 0.7×0.7 mm^2, taper off rapidly to the point of attachment to the cathode. The crystals can be conveniently separated from one another and the cathode by repeated, alternate washes in hot, dilute solutions of potassium carbonate and hydrochloric acid which also serve to dissolve the matrix.

Preliminary identification was carried out using a Rigaku D Max X-ray powder diffraction system. Graphite monochromatized copper radiation was employed. All lines of the pattern could be indexed on the basis of a tetragonal unit cell, similar to that reported by Torardi and McCarley (*4, 5*) for Na Mo_4O_6 with $a = 9.636(1)$ Å and $c = 2.879(1)$ Å. Electron microprobe analysis for K and Mo was carried out with a Jeol electron microprobe analysis system and confirmed the stoichiometry KMo_4O_6.

Structure Determination

Data for the structure determination were collected with a CAD4 Enraf–Nonius diffractometer. The experimental data and structure refinement parameters are summarized in Table I. A total of 1117 reflections with $I > 3\sigma(I)$ were used to refine the structure. Although Torardi and McCarley

TABLE I

DATA COLLECTION PARAMETERS

Empirical formula	KMo_4O_6
Formula weight	518.86
Crystal color	Black
Crystal system	Tetragonal
Crystal dimensions	0.5 × 0.12 × 0.12 mm^3
Lattice parameters	
a	9.636(1) Å
c	2.879(1) Å
Space group	$P\bar{4}$
Z	2
D_{calc}	6.44 g/cm^3
μ(Mo$K\alpha$)	97.1 cm^{-1}
Diffractometer	CAD4
Radiation	Mo$K\alpha$ (λ = 0.71069 Å)
Temperature	23°C
2θ	4–84°
Total number of reflections collected	1153
Number of independent reflections, $I > 3.00$(sig(I))	1117
Number of variables	36
Agreement factors (R_{zero})	0.034
Residuals: R, R_w	0.036, 0.040
Largest peak in final diff. map	2.8e/Å^3
Largest hole in the diff. map	3.0e/Å^3

(*4*) and Hoffman *et al.* (*11*) found that $NaMo_4O_6$ and the high-pressure form of KMo_4O_6 crystallize in space group $P4/mbm$ (No. 127), we found numerous violations of the *b* glide extinction rule. This and the compatibility of the atomic positions found for the above compounds led us to choose space group $P\bar{4}$ (No. 81). Since it seemed likely that the gross details of all structures were similar, the initial atomic parameters of the metal atoms chosen for refinements were those of $NaMo_4O_6$ taken from the work of Torardi (*5*). The positions of the oxygen atoms were subsequently determined by difference Fourier calculations. The least-squares refinement, carried out using the MOLEN crystallographic package, went smoothly to a final $R = 0.034$ ($R_w = 0.040$). The highest residual peak found in the final difference Fourier electron density analysis was 2.8 electrons/Å^3. Final positional and equivalent isotropic temperature factors are given in Table II. Anisotropic thermal parameters for K and Mo atoms are listed in Table III.

Electrical and Magnetic Measurements

Electrical resistivity measurements on selected crystals were made by a standard four-probe technique with a conventional liquid helium cryostat between 300 and 4 K. The prismatic crystals used in the resistivity measurements were initially washed with a warm 5% HF solution. Four copper leads were connected to indium fibers which were ultrasonically attached to selected faces of the crystal. The contacts were coated with silver paint to minimize contact resistance effects, if any. *I–V* characteristics were monitored periodically at different temperatures to ensure good quality of the contacts. Conductivity measurements on the smaller dimensions of the prism were carried out in a two-probe configuration. Magnetic susceptibility measurements were made with a Quantum Design SQUID magnetometer (MPMS system) at several temperatures in the range 2–390 K. The magnetization was measured at an applied magnetic field of 1000 G. The susceptibility values were corrected for the core diamagnetic contributions of the component ions.

Discussion

Structure

The structure of KMo_4O_6 found in this work bears a somewhat closer relationship to that of $NaMo_4O_6$ than do the other two forms of KMo_4O_6 reported by Hoffman *et al.* (*11*) based upon lattice type, bond lengths, and bond valence considerations. However, all contain the same basic structural unit consisting of chains of *trans*-edge-

TABLE II

ATOMIC COORDINATES FOR KMo_4O_6

Atom	Site	x	y	z	B_{eqv} (Å^2)
K(1)	1(*b*)	0	0	0.5	1.31(3)
K(2)	1(*d*)	0.5	0.5	0.5	1.29(3)
Mo(1)	4(*h*)	0.60105(4)	0.10101(4)	−0.0002(3)	0.347(4)
Mo(2)	4(*h*)	0.14276(4)	0.64262(4)	0.5069(3)	0.564(5)
O(1)	4(*h*)	0.2052(4)	0.2942(4)	0.494(3)	0.62(4)
O(2)	4(*h*)	0.2431(4)	0.0461(4)	−0.001(4)	0.63(4)
O(3)	4(*h*)	0.4545(4)	0.2568(4)	−0.010(4)	0.65(4)

sharing Mo_6 octahedra linked to one another through oxygen atoms to form tunnels in which the alkali metals reside in approximately cubic coordination as shown in Fig. 1. The Mo_6O_{12} cluster unit in KMo_4O_6 is shown in Fig. 2.

The existence of the structure depends largely on the stability of the metal oxygen framework. Indeed, sodium is too small to properly fit into the tunnels and as a result displays very long Na–O distances, 2.74 Å versus 2.54 Å, predicted by Shannon–Prewitt radii (*14*). On the other hand, when K^+ replaces Na^+, the volume of the cell undergoes only a small expansion to give K–O distances between 2.78 and 2.80 Å, somewhat smaller than the value of 2.87 Å predicted by Shannon–Prewitt radii (*14*).

The distance between alkali metals in all the tetragonal cages can be no longer than the c repeat distance, and as a result the K^+ ions are at 2.88 Å, disturbingly close to one another. However, similar distances have been observed in several transition metal oxides with the hollandite or hollandite-related structures, including $K_2Mo_8O_{16}$ (*15*). In this respect the longer c value of 2.95 Å found in the high-pressure form of KMo_4O_6 seems reasonable, although it is necessarily achieved by weakening the metal–metal bonding network within the chains. Interestingly the Mo–Mo distances (average distance 2.805 Å) in the *trans*-edge-sharing chains in the orthorhombic form [prepared *in vacuo* by a solid-state reaction (*6*)] are much closer to those (average distance 2.811 Å) found by us for the normal-pressure tetragonal form prepared by fused salt electrolysis than those (average distance 2.842 Å) found in the high-pressure tetragonal form (*11*). In the orthorhombic form the structural integrity of the chains is maintained. However, the K^+ ions are disordered on two sites which could result in the slightly longer average potassium distances observed.

TABLE III

GENERAL DISPLACEMENT PARAMETER EXPRESSIONS—U VALUES OF KMo_4O_6

Atom	$U(1,1)$	$U(2,2)$	$U(3,3)$	$U(1,2)$	$U(1,3)$	$U(2,3)$
K(1)	0.0157(6)	0.0157(6)	0.018(1)	0	0	0
K(2)	0.0160(6)	0.0160(6)	0.017(1)	0	0	0
Mo(1)	0.0042(1)	0.0042(1)	0.0048(1)	−0.0001(1)	−0.0004(3)	0.0005(3)
Mo(2)	0.0040(1)	0.0041(1)	0.0133(2)	−0.0002(1)	−0.0022(3)	−0.0017(3)

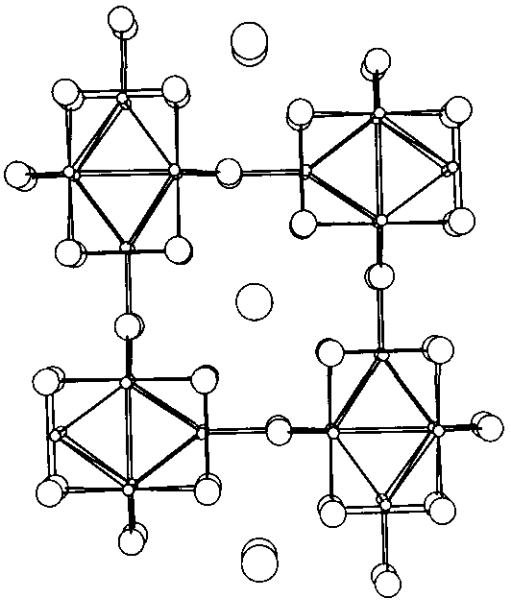

FIG. 1. Perspective view of the tetragonal KMo_4O_6 structure viewed along the c axis. The small and large open circles represent Mo and O atoms, respectively. The K^+ ions are shown as shaded circles.

We note two examples of reduced molybdenum compounds in which the substructure indicates the presence of strong cation–cation interactions. One is $Ba_{0.62}Mo_4O_6$ (*10*) and the other is $La_{1.16}Mo_8O_{16}$ (*16*). In the former, the subcell is identical with that found for the orthorhombic form of KMo_4O_6. However, extremely weak diffraction spots reveal a cell whose true c-axial length is eight times that of the subcell. This allows for an ordering of Ba^{2+} which eliminates strong cation–cation repulsions. In the case of the lanthanum compound, the average structure places the La^{3+} ions only 2.88 Å distant from one another. However, the true structure is found to be an incommensurate one in which La^{3+}–La^{3+} interactions are insignificant (*16*).

With these examples in mind, we examined overexposed oscillation photographs of our crystal of KMo_4O_6 for evidence of a longer c-axis repeat or the presence of spots indicative of incommensurate behavior and found no evidence for either. This would indicate that for similar cation–cation distances, repulsions between softer, singly charged potassium ions are less severe than for the harder, highly charged Ba^{2+} and La^{3+} species [8-coordinate Ba^{2+} is about 5% smaller than K^+, while trivalent lanthanum is about 20% smaller in radius (*14*)].

The polymorphic nature of KMo_4O_6 indicates that we are at or near the limits of stability for the tetragonal form prepared in this study and suggests that it is unlikely that $RbMo_4O_6$ could be formed without severely distorting the structure. While distortions of this structure have been observed, they occur, for the most part, for smaller, more covalent species and appear to be driven by the electron requirements of the Mo chains (*7, 12*).

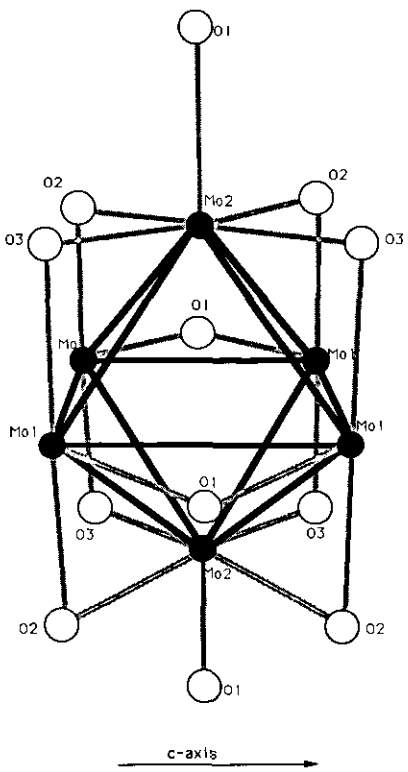

FIG. 2. Mo_6O_{12} cluster unit of the KMo_4O_6 structure.

TABLE IV

BOND VALENCE AND BOND ORDER SUMS FOR TETRAGONAL AMo_4O_6 (A = Na, K)

	KMo_4O_6 (this work)	KMo_4O_6 (ref. (*11*))	$NaMo_4O_6$ (ref. (*4*))
Mo–O bond valence Sum, s Mo(1)–O	2.44	2.41	2.46
Mo–O bond valence Sum, s Mo(2)–O	3.04	2.87	3.13
Σn_{Mo-Mo}	6.21	5.53	6.37
MCE per formula unit, $2\Sigma n_{Mo-Mo}$	12.4	11.1	12.8
From Mo–O bond valence sums	13.0	13.4	12.8
Number of valence electrons/Mo, $(N_e)_{Mo}$	5.85	5.40	5.98

A comparison of pertinent bond distances and bond orders for $NaMo_4O_6$ and the tetragonal forms of KMo_4O_6 are given in Tables IV and V, respectively. The Mo–Mo bond orders were calculated by the Pauling relationship between bond order and metal–metal bond length (*17*):

$$d(n) = d(1) - 0.6 \log n_{Mo-Mo}.$$

Here, $d(1)$ is the bond distance for a bond order of 1 and $d(n)$ is the observed bond distance corresponding to order n. A value of $d(1) = 2.614$ Å was used in these calculations (*7*). Mo–O bond valences, s, were calculated using the equation given by Brown and Wu (*18*):

$$s(\text{Mo–O}) = [d(\text{Mo–O})/1.882]^{-6.0}.$$

The value of N_e/Mo, the calculated number of valence electrons per Mo atom, is given by

$$(N_e)_{Mo} = 0.5\left[\sum s_{(Mo-O)} + \sum n_{Mo-Mo}\right].$$

A value of $(N_e)_{Mo}$ close to 6 is expected provided that the valence electrons are involved in either Mo–O or Mo–Mo bonding and that little localization of electrons in nonbonding orbitals takes place. This appears to be the case for the KMo_4O_6 form reported here and for $NaMo_4O_6$. However, the value of $(N_e)_{Mo} = 5.40$ for the high-pressure form of the potassium compound is anomalously low for this type of metal chain compound. Typical values are in the range 5.8–6.0 (*7*). The low $(N_e)_{Mo}$ value implies a significant degree of localization in this compound which could explain the significantly longer Mo–Mo distances along the c axis. Examination of the Σn_{Mo-Mo} values also supports this conclusion as do the metal cluster electron (MCE) counts from Mo–O bond valence sums (Table IV). Since the average oxidation number of Mo in AMo_4O_6 is 2.75 when A = alkali metal, up to $13e^-$ per formula unit should be available for Mo–Mo bonding. While the values of MCE for $NaMo_4O_6$ and KMo_4O_6 reported here give satisfactory agreement, the high-pressure form of KMo_4O_6 has a value of only 11.07, giving additional evidence for electron localization. In view of the long Mo–Mo distances (2.95 Å) along the axis of the chain, rather than describing the Mo–Mo bonding arrangement as a chain formed by *trans*-edge-sharing Mo_6 octahedra, one might more properly speak of two coaxial zig-zag chains of Mo which are crosslinked on alternate Mo.

Examination of the Mo–O bond distances in Table V for the most part show no large differences between the three compounds. This was somewhat surprising since the $P\bar{4}$ space group requires that the eightfold oxygen in $P4/mbm$ be split into two fourfold groups with independent x and y parameters, thus giving rise to the possibility of

TABLE V

COMPARISON OF BOND DISTANCES (Å) IN THE NORMAL AND HIGH-PRESSURE TETRAGONAL FORMS OF KMo_4O_6 AND $NaMo_4O_6$

Bond	KMo_4O_6[a]	KMo_4O_6[b]	$NaMo_4O_6$[c]
Mo(1)–Mo(1)	2.879(1) [2×][d]	2.950(1) [2×]	2.862(0) [2×]
Mo(1)–Mo(1)	2.754(1)	2.759(1)	2.753(3)
Mo(1)–Mo(2)	2.794(1) [2×]	2.809(1) [8×]	2.780(2) [8×]
Mo(1)–Mo(2)	2.774(1) [2×]		
Mo(1)–Mo(2)	2.793(1) [2×]		
Mo(1)–Mo(2)	2.773(1) [2×]		
Mo(2)–Mo(2)	2.879(1) [2×]	2.950(1) [2×]	2.862(0) [2×]
Mo(1)–O(1)	2.013(6)	2.041(6) [2×]	2.015(8) [2×]
Mo(1)–O(1)	2.037(6)		
Mo(1)–O(2)	2.066(4)	2.055(8) [2×]	2.068(8) [2×]
Mo(1)–O(3)	2.061(4)		
Mo(2)–O(1)	2.069(4)	2.054(9)	2.024(11)
Mo(2)–O(2)	2.049(9)	2.066(6) [4×]	2.040(6) [4×]
Mo(2)–O(2)	2.027(9)		
Mo(2)–O(3)	2.033(9)		
Mo(2)–O(3)	2.045(9)		
K(1)–O(2)	2.783(7) [4×]	2.794(7) [8×]	2.742(8) [8×]
K(2)–O(2)	2.787(7) [4×]		
K(2)–O(3)	2.800(7) [4×]	2.794(7) [8×]	2.742(8) [8×]
K(2)–O(3)	2.770(7) [4×]		

[a] This work. ESDs are given in parentheses.
[b] Reference (*11*).
[c] Reference (5).
[d] Bond multiplicities are given in square brackets.

significant bond distance shifts. For the most part this was not seen except for a nearly 0.05-Å increase in the Mo(2)–O(1) distance in the K compound reported here as compared to the Na isotype. Since O(1) is involved in interchain bonding, changes in this distance will strongly influence the contributions of Mo–O d–p π overlap to the overall bonding scheme. One might also have expected that O(2) and O(3) might move significantly as compared to the sodium compound so as to provide a longer K–O distance closer to that predicted by Shannon–Prewitt radii (*14*). In fact this did happen to some extent. If one calculates the K–O distances that would have been obtained in KMo_4O_6, if it had the same atom positional parameters as $NaMo_4O_6$, the average increase would be about 0.03 Å. That a larger increase did not take place implies that electrostatic repulsions between neighboring K^+ are effectively shielded by increased K–O interactions.

Physical Properties

The electrical resistivity measured along the crystallographic c axis of KMo_4O_6 as a function of temperature is shown in Fig. 3. The decrease in the electrical resistivity with temperature in the range 120–300 K is indicative of metallic behavior, while a transition to semiconducting behavior is evident below ~120 K. As can be seen the transition is fairly broad and is observed in different measurements on several crystals. The room temperature resistivity along the

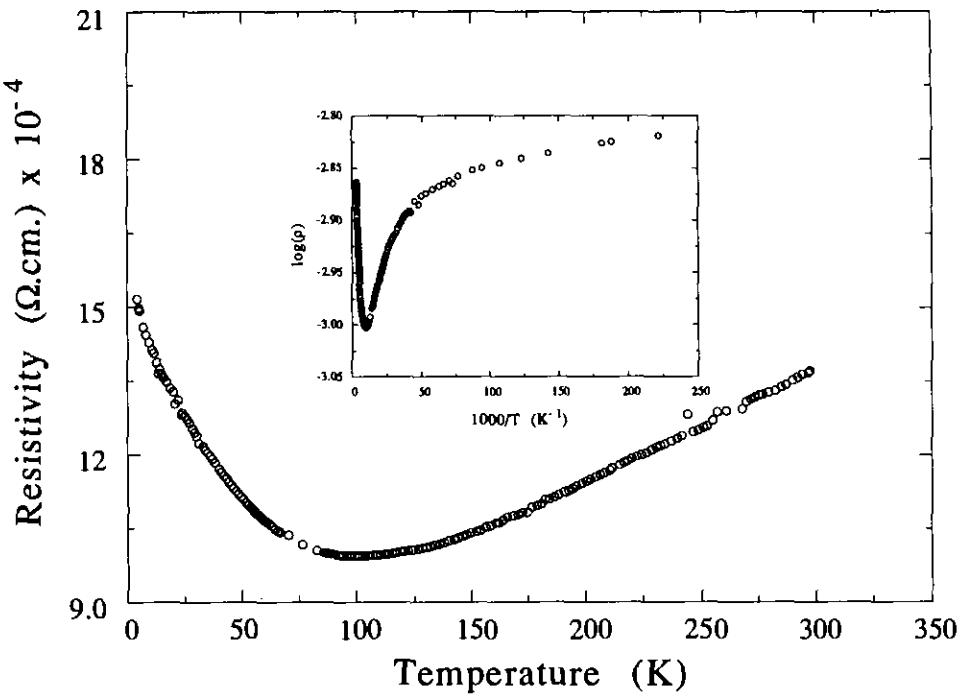

FIG. 3. Variation of electrical resistivity along the c axis of KMo_4O_6 single crystal as a function of temperature. Inset: the log (ρ) vs 1000/T plot.

direction of the *trans*-edge-sharing chains of Mo octahedra is $\sim 1.3 \times 10^{-3}$ ohm · cm. The resistivity perpendicular to these chains (i.e., in the tetragonal basal plane) could not be measured in a four-probe configuration on account of the small dimensions of the crystals; however, using a two-probe measurement, the room temperature resistivity is estimated to be $\sim 4 \times 10^{-3}$ ohm · cm. The temperature dependence of the electrical resistivity measured in the *ab* plane remained metallic down to 2 K with no apparent transition to semiconducting behavior. The observation that the room temperature electrical resistivity values measured along and perpendicular to the c axis are within an order of magnitude seems to indicate significant delocalization of the carriers between the chains, consistent with the structural considerations discussed above.

Magnetic susceptibility as a function of temperature on two batches of single crystals, one randomly oriented and the other oriented along the chains of Mo_6 octahedra, is presented in Fig. 4. The total susceptibility was corrected for the core diamagnetic contributions from the component ions. It is evident from this plot that the susceptibility remains nearly temperature independent and indicates Pauli paramagnetism which is consistent with the observed metallic behavior. It is interesting to note that there is no anomaly in the magnetic susceptibility at the temperature corresponding to the metal–semiconductor transition observed in the electrical resistivity measurements. This implies that the origin of metal–semiconductor transition in KMo_4O_6 is not likely to be magnetic in nature. The low-temperature upturns observed in the χ vs T plots (Fig. 4) could be attributed to the presence of small amounts of magnetic impurities in the crystals.

McCarley *et al.* (*19*) have reported the

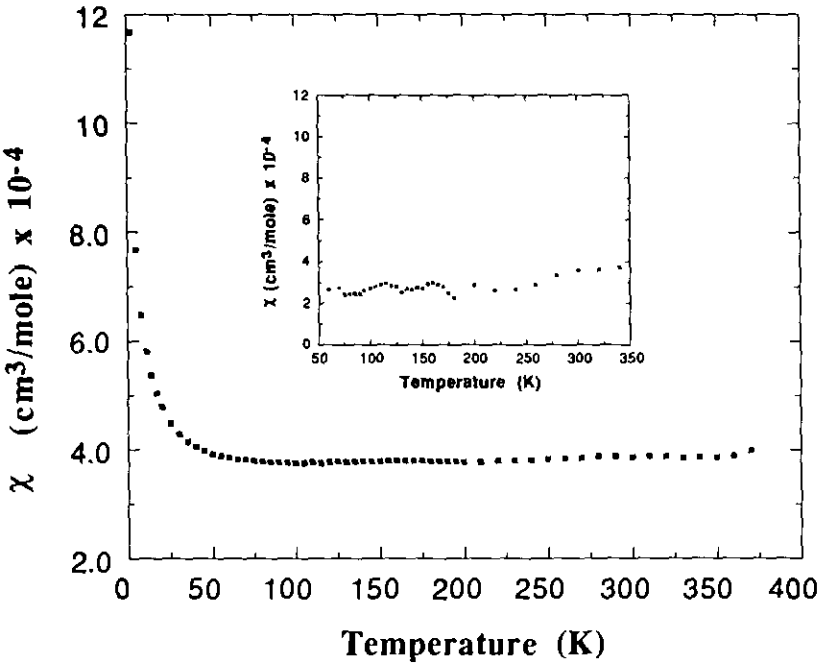

FIG. 4. Temperature dependence of the magnetic susceptibility for a collection of randomly oriented KMo_4O_6 crystals. Inset: susceptibility as a function of temperature measured with the applied field parallel to the tetragonal c axis.

room temperature electrical resistivity of $NaMo_4O_6$ single crystals to be $\sim 10^{-4}$ ohm · cm. The temperature dependence of the electrical resistivity measured on pressed pellets of $NaMo_4O_6$, however, revealed a semiconducting behavior with a rapid increase in the resistivity below 100 K. Furthermore, the resistivity below 10 K showed an anomalous drop which has been attributed to a structural phase transition. Although our results on the single-crystal electrical resistivity of KMo_4O_6 are consistent with the upturn in the resistivity at ~100 K observed for $NaMo_4O_6$, no evidence of a sudden decrease in the resistivity was observed at low temperatures. The thermal activation energies for the electrical conduction along the crystallographic c axis below 100 K were calculated from the Arrhenius plots shown in Fig. 2. Clearly, the log ρ vs $1/T$ plot (inset to Fig. 3) shows two distinct slopes, which indicate a change in the conduction mechanism. The low activation energy (5.8×10^{-5} eV) in the temperature interval 2–10 K is consistent with an extrinsic type of behavior. However, the E_a of 1.0×10^{-3} eV in the range 40–90 K could be attributed to either Anderson-type localization effects or a possible order–disorder type of structural transition as has been proposed for $NaMo_4O_6$ (*20*).

Acknowledgments

The authors thank Professor H. J. Schugar and S. Ginell for their help with single-crystal X-ray data collection. Helpful discussions with Professor J. Potenza, Dr. S. -C. Chen, Dr. R. L. Fuller, and Dr. M. Greaney are gratefully acknowledged. The work was supported by National Science Foundation Solid State Chemistry Grants DMR-8842788 and DMR-9019301.

References

1. M. GREENBLATT, *Chem. Rev.* **88,** 31 (1988).
2. A. WOLD AND D. BELLEVANCE, "Preparative Methods in Solid State Chemistry" (P. Hagenmuller, Ed.), pp. 279–308, Academic Press, New York (1972).

3. W. H. McCarroll and M. Greenblatt, *J. Solid State Chem.* **54,** 282 (1984).
4. C. C. Torardi and R. E. McCarley, *J. Am. Chem. Soc.* **101,** 3963 (1979).
5. C. C. Torardi, Ph.D. thesis, Iowa State University, Ames (1981).
6. C. C. Torardi and R. E. McCarley, *J. Solid State Chem.* **37,** 393 (1981).
7. R. E. McCarley, *Polyhedron* **5,** 51 (1986).
8. R. E. McCarley, "Inorganic Chemistry: Toward the 21st Century" (M. H. Chisholm, Ed.), ACS Symp. Ser. 211, pp. 274–290. ACS, Washington, DC (1983).
9. R. E. McCarley, K-H. Lii, P. A. Edwards, and L. F. Brough, *J. Solid State Chem.* **57,** 17 (1985).
10. C. C. Torardi and R. E. McCarley, *J. Less Common Met.* **116,** 169 (1986).
11. R. Hoffman, R. Hoppe, K. Bauer, and K.-J. Range, *J. Less Common Met.* **161,** 279 (1990).
12. T. Hughbanks and R. Hoffmann, *J. Am. Chem. Soc.* **105,** 3528 (1983).
13. A. wold, W. Kunnmann, R. J. Arnott, and A. Ferretti, *Inorg. Chem.* **3,** 545 (1964).
14. R. D. Shannon, *Acta Crystallogr. A* **32,** 751 (1976).
15. C. C. Torardi and J. C. Calabrese, *Inorg. Chem.* **23,** 3281 (1984).
16. H. LeLigny, Ph. Labbe, M. Ledesert, B. Raveau, C. Valdez, and W. H. McCarroll, *Acta Crystallogr. B* **48,** 134 (1992).
17. L. Pauling, "The Nature of the Chemical Bond," 3rd ed., p. 400, Cornell Univ. Press, Ithaca, NY (1960).
18. I. D. Brown and K. K. Wu, *Acta Crystallogr. B* **32,** 1957 (1976).
19. R. E. McCarley, T. R. Ryan, and C. C. Torardi, "Reactivity of Metal–Metal Bonds" (M. H. Chisholm, Ed.), ACS Symp. Ser. 155, p. 41, ACS, Washington, DC (1981).
20. P. J. Chu and B. C. Gerstein, *J. Chem. Phys.* **90,** 3713 (1989).